1103 (1969).
[4]D. Schoemaker and J. L. Kolopus, Phys. Rev. B 2, 1148 (1970).
[5]G. Guiliani, Phys. Rev. B 2, 464 (1970).
[6]N. Itoh and M. Saidoh, Phys. Status Solidi 33, 649 (1969); M. Saidoh and N. Itoh, Phys. Letters 31A, 68 (1970).
[7]G. J. Dienes, R. D. Hatcher, and R. Smoluchowski, Phys. Rev. 157, 692 (1967); R. D. Hatcher, W. D. Wilson, R. Smoluchowski, and G. J. Dienes, Bull. Am. Phys. Soc. 14, 324 (1969).
[8]N. E. Byer and H. S. Sack, J. Phys. Chem. Solids 29, 677 (1968).
[9]T. G. Castner and W. Känzig, J. Phys. Chem. Solids 3, 178 (1957); T. O. Woodruff and W. Känzig, *ibid.* 5, 268 (1958).
[10]C. J. Delbecq, B. Smaller, and P. H. Yuster, Phys. Rev. 111, 1235 (1958); C. J. Delbecq, W. Hayes, and P. H. Yuster, *ibid.* 121, 1043 (1961).
[11]D. Schoemaker, in Proceedings of the International Symposium on Color Centers in Alkali Halides, University of Illinois, Urbana, 1965, Abstract No. 167 (unpublished).
[12]I. L. Bass and R. L. Mieher, Phys. Rev. 175, 421 (1968).
[13]F. W. Patten and F. J. Keller, Phys. Rev. 187, 1120 (1969).
[14]In a recent attempt to test the Pooley-Hersh mechanism of color-center formation by F. J. Keller and F. W. Patten [(Solid State Commun. 7, 1603 (1969)] it was concluded that recombination of an electron with a V_K-type center (Cl_2^- or $ClBr^-$) may result in interstitial Cl atom formation. However, at the high temperatures we are working at, we observe only the decay of Cl_2^-, without a detectable increase in the concentration of the interstitial centers.
[15]The interstitial Cl ions Cl_i^- are not paramagnetic, and their behavior cannot be studied directly with EPR. The trapped Cl_i^-, called the *I* center, is unstable at 77 K in KCl, but there is evidence from the optical-absorption measurements (Refs. 6 and 7) that a mobile interstitial halogen ion, just like a mobile interstitial halogen atom, may be trapped by Na^+ or Li^+ ions forming what one could call $I_A(Na^+)$ or $I_A(Li^+)$ centers. It seems reasonable to expect that Cl_i^- may also be stabilized up to an even higher temperature by pairs of Na^+ or Li^+ ions, producing I_{AA} and/or $I_{A'A}$ centers.
[16]W. Hayes and J. W. Hodby, Proc. Roy. Soc. (London) 294A, 359 (1966).
[17]D. Schoemaker, Bull. Am. Phys. Soc. 12, 410 (1967).
[18]W. Hayes and G. M. Nichols, Phys. Rev. 117, 993 (1960).
[19]C. J. Delbecq, D. Schoemaker, and P. H. Yuster, Phys. Rev. B 3, 473 (1971).
[20]However, it is quite possible that such a center might be produced by x or γ irradiation at temperatures below 77 K.
[21]K. Bachmann and H. Peisl, J. Phys. Chem. Solids 31, 1525 (1970).
[22]If the distribution of the Li^+ or Na^+ ions were random, and if the cross section for trapping interstitial Cl atoms were the same for both the nn and nnn pairs, then the $H_{A'A}/H_{AA}$ concentration ratio should be exactly 2. The large difference in appearance and relaxation behavior of these centers does not allow one to determine this ratio accurately. One can only say that H_{AA} and $H_{A'A}$ have comparable concentrations.
[23]H. M. McConnell, J. Chem. Phys. 25, 709 (1956).
[24]G. E. Pake, *Paramagnetic Resonance* (Benjamin, New York, 1962).
[25]A recent paper in the field of motional effects in EPR which, apart from treating a simple case in detail, gives some representative references in this field is R. C. Hughes and Z. G. Soos, J. Chem. Phys. 52, 6302 (1970).
[26]K. Bachmann and W. Känzig, Physik Kondensierten Materie 7, 286 (1968).
[27]D. Schoemaker and E. L. Yasaitis, Bull. Am. Phys. Soc. 16, 440 (1971).

PHYSICAL REVIEW B VOLUME 3, NUMBER 10 15 MAY 1971

Resonant Phonon-Assisted Generation of Second-Harmonic Light

P. N. Keating and C h. Deutsch*
Bendix Research Laboratories, Southfield, Michigan 48075
(Received 25 November 1970)

The generation of second-harmonic optical radiation with the simultaneous absorption or stimulated emission of acoustical phonons is studied both theoretically and experimentally. A quantum theory of the processes involved is developed on the basis of perturbation theory. The analysis predicts that a multiple resonance in the output power should be observable as a function of the acoustical propagation angle for propagation close to normal to the fundamental optical beam. Experimental results are presented in which a double resonance peak is observed for 1.06-μ input optical radiation and 300-MHz longitudinal acoustical radiation in $LiNbO_3$. The observed angular separation between the two peaks agrees well with that expected for phonon-absorption and -emission contributions from a pole in the scattering amplitude at twice the fundamental optical frequency.

I. INTRODUCTION

The generation of optical harmonics by mixing intense light beams in optically nonlinear crystals has become a relatively common technique since the original classic work of Franken *et al.*[1] One

recent development in this field is the introduction of acoustic radiation to induce the nonlinear process.[2,3] In essence, the wave vector of the acoustic phonon is added into the wave-vector conservation (or "index-matching") requirements to allow index matching to occur for optical radiation for which the usual birefringent index matching is not possible. Then, for example, nonlinear optical processes are possible in cubic crystals such as GaAs,[3] which are not birefringent. Furthermore, if phonon-assisted (or "acoustically induced") nonlinear processes can be made efficient enough, rapid acoustical tuning of parametric oscillators becomes possible.

In addition to the experimental results on GaAs, Boyd *et al.*[3] have given a classical description of the effect, which has been considerably extended by Nelson and Lax.[4] In the present article, we present (a) a quantum-theoretical treatment of phonon-assisted second-harmonic generation (SHG) and (b) experimental results obtained in $LiNbO_3$ which verify some of the theoretical results. Section II contains a quantum-perturbation theory of the more important processes which contribute to phonon-assisted SHG. Section III consists of a discussion of these theoretical results, with emphasis on the resonances to be expected. In Sec. IV, we present an account of an experimental study in which a double resonance peak is observed.

II. THEORY

Classical theories of phonon-assisted (or acoustically induced) SHG have been given by Boyd *et al.*[3] and Nelson and Lax.[4] In this section, we present a quantum-theoretical approach to the effect which provides additional results and insight. The approach utilizes time-dependent nonrelativistic perturbation theory up to second order and is based to some extent on the work of She.[5]

Nelson and Lax[4] have considered a number of classical processes which contribute to the phonon-assisted effect and which have quantum equivalents. Two of the processes are essentially the same and occur in third order; they will not be included here. A third process involves third-order optical nonlinearity and will also be excluded, on the grounds that third-order nonlinear effects are generally of lesser importance in crystals without inversion symmetry. Although these exclusions are made in order to avoid unwieldy analysis, the present theory may readily be generalized to include them. In their analysis, Nelson and Lax[4] have considered the anisotropy of the various classical tensors in appreciable detail. No such attempt will be made here to examine the anisotropy effects. Instead, we shall emphasize the quantum approach and especially the contribution which arises in second-order perturbation theory.

The interactions which are included in the Hamiltonian density, in addition to the free-field photon and phonon terms, are

$$\mathcal{H}_I = \mathcal{H}_1 + \mathcal{H}_2 + \mathcal{H}_3 ,$$

where

$$\mathcal{H}_1(x) = \frac{1}{V^2} \sum_{k_1 k_2 k_3 q} B_{k_1 k_2 k_3 q}\, a^\dagger_{k_1} a_{k_2} a_{k_3} b_q e^{i(k_1 - k_2 - k_3 - q)\cdot x} + \text{H. c.} \tag{1}$$

is the direct term, and will give a contribution in first order which is analogous to contribution (1) of Nelson and Lax[4];

$$\mathcal{H}_2(x) = \frac{1}{V^{3/2}} \sum_{k_1 k_2 k_3} C_{k_1 k_2 k_3}\, a^\dagger_{k_1} a_{k_2} a_{k_3}\, e^{i(k_1 - k_2 - k_3)\cdot x} + \text{H. c.} \tag{2}$$

is the second-order nonlinear interaction and gives, for example, the usual SHG[1]; and

$$\mathcal{H}_3(x) = \frac{1}{V^{3/2}} \sum_{k_1 k_2 q} D_{k_1 k_2 q}\, a^\dagger_{k_1} a_{k_2} b_q\, e^{i(k_1 - k_2 - q)\cdot x} + \text{H. c.} \tag{3}$$

is the interaction which gives rise to Brillouin scattering, for example, and corresponds classically to the acousto-optic effect. In these expressions, k, q, and x are four-vectors in Lorentz space with contravariant components given by $k^\mu = (\vec{k}, \omega_{\vec{k}}/c)$, $q^\mu = (\vec{q}, \Omega_{\vec{q}}/c)$, $x^\mu = (\vec{x}, ct)$, and $k \cdot x$ is the usual scalar product $k^\mu x_\mu = \omega t - \vec{k}\cdot\vec{x}$ of Lorentz space. The a_k, b_q are the field amplitudes for photons and acoustic phonons, respectively, and satisfy the usual boson commutation relations. The three-vectors $\vec{k}$ and $\vec{q}$ are the wave vectors in the crystal and $\omega_{\vec{k}}$, $\Omega_{\vec{q}}$ are the solutions of the dispersion equations $\omega = \omega_\lambda(\vec{k})$ and $\Omega = \Omega_j(\vec{q})$. The volume V is the normalization volume.

The scattering operator is a function of the integral

$$\int \mathcal{H}_1(x)\, dx^4 = \frac{1}{c_t V^{3/2}} \left(\frac{1}{V^{1/2}} \sum B_{k_1 k_2 k_3 q}\, a^\dagger_{k_1} a_{k_2} a_{k_3} b_q\, [vlf(\Delta\vec{k})]\, \delta_{\omega_1, \omega_2, \omega_3 + \Omega} \right.$$

$$\left. + \sum C_{k_1 k_2 k_3}\, a^\dagger_{k_1} a_{k_2} a_{k_3}\, [LVF(\Delta\vec{k}')]\, \delta_{\omega_1, \omega_2 + \omega_3} + \sum D_{k_1 k_2 q}\, a^\dagger_{k_1} a_{k_2} b_q\, [vlf(\Delta\vec{k}'')]\, \delta_{\omega_1, \omega_2 + \Omega} \right) , \tag{4}$$

where ω_1 represents $\omega_{\vec{k}_1}$ and Ω represents $\Omega_{\vec{q}}$. In this expression, v is the interaction volume, l/c_l and L/c_l are the transit times for light through the acousto-optic interaction region and the crystal, respectively, and $f(\vec{\kappa})$, $F(\vec{\kappa})$ are the dimensionless "spread functions" corresponding to incomplete "index matching" within the interaction and normalization volumes, respectively. The arguments are

$$\begin{aligned}\Delta\vec{k} &= \vec{k}_1 - (\vec{k}_2 + \vec{k}_3 + \vec{q}) \ , \\ \Delta\vec{k}' &= \vec{k}_1 - (\vec{k}_2 + \vec{k}_3) \ , \\ \Delta\vec{k}'' &= \vec{k}_1 - (\vec{k}_2 + \vec{q}) \ .\end{aligned} \tag{5}$$

In order to relate the present analysis more readily to conventional processes, we shall carry out a brief treatment of the usual SHG and Brillouin scattering, as well as analyzing first- and second-order contributions to phonon-assisted SHG.

A. First-Order Processes

Assuming an initial state of n_k photons in one mode, the state which is generated by the interaction is

$$S|i\rangle = \exp[-(i/\hbar)\int dx^4\ \mathcal{H}_1(x)]|n_k\rangle \tag{6}$$

in the interaction representation. The operator S is the scattering operator $U(\infty, -\infty)$. For the unassisted SHG, the final-state amplitude of interest is, from Eq. (4),

$$|f\rangle = \frac{-i}{\hbar}\frac{L}{V^{1/2}c_l} C_{k_1kk}[n_k(n_k-1)]^{1/2} \times \delta_{\omega_1,2\omega} F(\vec{k}_1 - 2\vec{k}) a^\dagger_{k_1}|n_k - 2\rangle \tag{7}$$

in lowest order. The expected number of final photons in mode k_1 is

$$\langle n_{k_1}\rangle = \langle f|a^\dagger_{k_1}a_{k_1}|f\rangle = \frac{L^2}{\hbar^2 V c_l^2}|C_{k_1kk}|^2 n_k(n_k-1)|F(\vec{k}_1 - 2\vec{k})|^2\delta_{\omega_1,2\omega} \ . \tag{8}$$

We can relate this to the power density (i.e., power per unit area) P generated in the classical limit $n_k \gg 1$ via the relation

$$P_k = \hbar\omega_k c_l n_k / V \ . \tag{9}$$

Thus

$$P_{k_1} \cong \frac{2}{\hbar^3 c_l^3 \omega_{\vec{k}}}|C_{k_1kk}|^2 L^2 P_k^2 |F(\vec{k}_1 - 2\vec{k})|^2 \delta_{\omega_{\vec{k}_1},2\omega_{\vec{k}}} \tag{10}$$

in the classical limit, which is in agreement with the previous work.[6]

Similarly, for Brillouin scattering, the final-state amplitudes of interest generated from an initial state $|n_k, m_q\rangle$ are

$$|f_a\rangle = \frac{-i}{\hbar}\frac{vl}{V^{3/2}c_l} D_{k_1kq}(n_k m_q)^{1/2} \times f(\Delta\vec{\kappa})\,\delta_{\omega_1,\omega+\Omega}\, a^\dagger_{k_1}|n_k - 1,\ m_q - 1\rangle \ , \tag{11}$$

$$|f_e\rangle = \frac{-i}{\hbar}\frac{vl}{V^{3/2}c_l} D^*_{kk'_1q}[n_k(m_q+1)]^{1/2} \times f(\Delta\vec{\kappa}')\,\delta_{\omega'_1,\omega-\Omega}\ a^\dagger_{k'_1}|n_k - 1, m_q + 1\rangle$$

(where ω'_1 represents $\omega_{\vec{k}'_1}$, etc., and ω represents $\omega_{\vec{k}}$) for absorption and (stimulated) emission of phonons, respectively, where

$$\begin{aligned}\Delta\vec{\kappa} &= \vec{k}_1 - \vec{k} - \vec{q} \ , \\ \Delta\vec{\kappa}' &= \vec{k}'_1 - \vec{k} + \vec{q} \ .\end{aligned} \tag{12}$$

In the classical limit $n_k \gg 1$, $m_q \gg 1$, we obtain

$$P^a_{k_1} = \frac{l^2}{\hbar^3\Omega_{\vec{q}}c_a c_l^2}\left(\frac{\omega_{\vec{k}}+\Omega_{\vec{q}}}{\omega_{\vec{k}}}\right)\left(\frac{v}{V}\right)^2 \times P_k P_q |D_{k_1kq}|^2 |f(\vec{k}_1 - \vec{k} - \vec{q})|^2\,\delta_{\omega_{\vec{k}_1},\omega_{\vec{k}}+\Omega_{\vec{q}}} \ , \tag{13}$$

and a very similar result for the power density $P^e_{k_1}$, corresponding to phonon emission.

Under the conditions when phonon-assisted SHG is possible, both of the processes discussed above (i.e., via $\mathcal{H}_2$, $\mathcal{H}_3$) also occur and the result of their *consecutive* occurrence is essentially the same as that of the phonon-assisted process of interest, except in magnitude. The power density generated (via phonon absorption) by the consecutive events is

$$P_{k_1} = \left(\frac{2\omega_{\vec{k}}+\Omega_{\vec{q}}}{\omega_{\vec{k}}}\right)\frac{l^2}{\hbar^6\omega_{\vec{k}}\Omega_{\vec{q}}c_l^3 c_a}\left(\frac{v}{V}\right)^2 \times P_k^2 P_q\,(|A_{k_1}|^2 + |A'_{k_1}|^2)\,\delta_{\omega_{\vec{k}_1},2\omega_{\vec{k}}+\Omega_{\vec{q}}} \ , \tag{14}$$

where the two terms corresponding to the two cases of (i) Brillouin scattering first and (ii) SHG first are given by

$$A_{k_1} = \frac{L}{c_l}\sum_{k'} C_{k_1k'k}D_{k'kq} \times F(\vec{k}_1 - \vec{k}' - \vec{k})\, f(\vec{k}' - \vec{k} - \vec{q})\,\delta_{\omega_{\vec{k}'},\omega_{\vec{k}}+\Omega_{\vec{q}}} \ , \tag{15}$$

$$A'_{k_1} = \frac{L}{c_l}\sum_{k'} C_{k'kk}D_{k_1k'q} \times F(\vec{k}' - 2\vec{k})\, f(\vec{k}_1 - \vec{k}' - \vec{q})\,\delta_{\omega_{\vec{k}'},2\omega_{\vec{k}}} \ .$$

In addition, there is an expression similar to Eq. (14) for the case of stimulated phonon emission.

The relationship between this uninteresting consecutive process and the more interesting phonon-

assisted generation process will be discussed further in Sec. III.

We have yet to discuss any of the phonon-assisted processes which are of direct interest here. Only one such process occurs in first order, via the interaction $\mathcal{H}_1$. In this case,

$$\langle n_{\vec{k}_1}\rangle = \frac{v^2 l^2}{\hbar^2 V^4 c_l^2}\,|B_{k_1 k k q}|^2 [n_k m_q (n_k - 1)] \times |f(\vec{k}_1 - 2\vec{k} - \vec{q})|^2\, \delta_{\omega_{\vec{k}_1}, 2\omega_{\vec{k}} + \Omega_{\vec{q}}} \quad (16)$$

for the absorption process, with a similar result for stimulated phonon emission. Therefore, in the classical limit, the power density generated via the phonon-absorption process, is

$$P_{\vec{k}_1} = \frac{l^2}{\hbar^4 \omega_{\vec{k}} \Omega_{\vec{q}} c_l^3 c_a}\left(\frac{2\omega_{\vec{k}} + \Omega_{\vec{q}}}{\omega_{\vec{k}}}\right)\left(\frac{v}{V}\right)^2 |B_{k_1 k k q}|^2 \times P_k^2 P_q |f(\vec{k}_1 - 2\vec{k} - \vec{q})|^2\, \delta_{\omega_{\vec{k}_1}, 2\omega_{\vec{k}} + \Omega_{\vec{q}}}\ , \quad (17)$$

with a similar result for phonon emission.

B. Second-Order Processes

In Sec. II A, two processes which must be taken into account were considered: (i) the direct phonon-assisted SHG process, via $\mathcal{H}_1$, and (ii) the consecutive Brillouin scattering and conventional SHG events. The former is a process which is of direct interest, whereas the latter is not a true phonon-assisted process at all. It must, however, be considered because it can give a final photon state which is essentially the same as that given by the phonon-assisted processes.

With the present Hamiltonian, the second-order process of interest is that in which both $\mathcal{H}_2$ and $\mathcal{H}_3$ take part. In this respect, it is somewhat similar to the consecutive Brillouin and SHG process described in Sec. II A. It differs from it, of course, in an important way, i.e., in the nature of the intermediate particle in the interaction. In the consecutive process discussed above, the intermediate state is a real state, whereas in the contemporaneous process treated in second-order perturbation theory below, the intermediate state is, of course, a virtual-photon state.

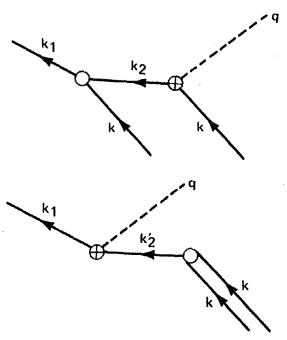

FIG. 1. Two diagrams representing contributions to phonon-assisted second-harmonic generation (phonon absorption) in second-order perturbation theory. The full lines are photon lines and the broken ones are phonon lines.

In second-order, the final state is

$$\tfrac{1}{2}(-i/\hbar)^2 \int d^4x\, d^4x'\, T\{\mathcal{H}_I(x)\mathcal{H}_I(x')\}|i\rangle\ , \quad (18)$$

where T is the Wick time-ordering operator. For the moment, we shall confine ourselves only to phonon-absorption processes, so that the initial state is $|n_k, m_q\rangle$ and the final state of interest is $a^\dagger_{k_1}|n_k - 2, m_q - 1\rangle$. Thus, we are interested in the two different contributions to Eq. (18) which are represented in Fig. 1. With the help of Wick's theorem,[7] the first of these gives

$$\left(\frac{-i}{\hbar}\right)^2 \sum_{k_2} C_{k_1 k_2 k} D_{k_2 k q} \frac{v}{V^2} F(\Delta\vec{k}_1) f(\Delta\vec{k}_2) \frac{l}{c_l}\, \delta_{\omega_{\vec{k}_1}, 2\omega_{\vec{k}} + \Omega_{\vec{q}}} \times \int d\tau\, \langle a^\cdot_{k_2}(\tau) a^{\dagger\cdot}_{k_2}(0)\rangle e^{i(\omega_{\vec{k}} + \Omega_{\vec{q}})\tau} a^\dagger_{k_1} a_k a_k b_q |i\rangle\ , \quad (19)$$

where

$$\Delta\vec{k}_1 = \vec{k}_1 - \vec{k}_2 - \vec{k}\ , \qquad \Delta\vec{k}_2 = \vec{k}_2 - \vec{k} - \vec{q}$$

and where the pair of dots in the bracket denotes a Wick product. Hence, the final-state amplitude of interest is

$$|f_a\rangle = \frac{-ivl}{\hbar^2 V^2 c_l} \sum_{k_2} C_{k_1 k_2 k} D_{k_2 k q} F(\Delta\vec{k}_1) \times f(\Delta\vec{k}_2)[m_q n_k (n_k - 1)]^{1/2}\, \delta_{\omega_{\vec{k}_1}, 2\omega_{\vec{k}} + \Omega_{\vec{q}}} \times \frac{2\omega_{\vec{k}_2}}{(\omega_{\vec{k}_2})^2 - (\omega_{\vec{k}} + \Omega_{\vec{q}})^2} a^\dagger_{k_1} |n_k - 2, m_q - 1\rangle\ . \quad (20)$$

In addition, we have another phonon-absorption contribution, represented by the second diagram in Fig. 1:

$$|f'_a\rangle = \frac{-ivl}{\hbar^2 V^2 c_l} \sum_{k'_2} C_{k'_2 k k} D_{k_1 k'_2 q} F(\Delta\vec{k}'_2) \times f(\Delta\vec{k}'_1)[m_q n_k (n_k - 1)]^{1/2}\, \delta_{\omega_{\vec{k}_1}, 2\omega_{\vec{k}} + \Omega_{\vec{q}}} \times \frac{2\omega_{\vec{k}'_2}}{(\omega_{\vec{k}'_2})^2 - (2\omega_{\vec{k}})^2} a^\dagger_{k_1} |n_k - 2, m_q - 1\rangle\ , \quad (21)$$

where $\Delta\vec{k}'_1 = \vec{k}_1 - \vec{k}'_2 - \vec{q}$, $\Delta\vec{k}'_2 = \vec{k}'_2 - 2\vec{k}$. The two contributions, when taken together, give a classical generated power density of

$$P^A_{\vec{k}_1} = \left(\frac{2\omega_{\vec{k}} + \Omega_{\vec{q}}}{\omega_{\vec{k}}}\right) \frac{l^2}{\hbar^6 \omega_{\vec{k}} \Omega_{\vec{q}} c_l^3 c_a} \left(\frac{v}{V}\right)^2 \times P_k^2 P_q |M^A_{k_1} + M'^A_{k_1}|^2\, \delta_{\omega_{\vec{k}_1}, 2\omega_{\vec{k}} + \Omega_{\vec{q}}}\ , \quad (22)$$

where

$$M^{A}_{\vec{k}_1} = \sum_{\vec{k}_2} \frac{2\omega_{\vec{k}_2} C_{\vec{k}_1\vec{k}_2\vec{k}} D_{\vec{k}_2\vec{k}\vec{q}}}{(\omega_{\vec{k}_2})^2 - (\omega_{\vec{k}} + \Omega_{\vec{q}})^2} F(\vec{k}_1 - \vec{k}_2 - \vec{k}) f(\vec{k}_2 - \vec{k} - \vec{q}) , \tag{23}$$

$$M'^{A}_{\vec{k}_1} = \sum_{\vec{k}_2'} \frac{2\omega_{\vec{k}_2} C_{\vec{k}_2'\vec{k}\vec{k}} D_{\vec{k}_1\vec{k}_2'\vec{q}}}{(\omega_{\vec{k}_2})^2 - (2\omega_{\vec{k}})^2} F(\vec{k}_2' - 2\vec{k}) f(\vec{k}_1 - \vec{k}_2' - \vec{q}) .$$

Similarly, when $m_q \gg 1$, the power density generated via the stimulated phonon-emission process is

$$P^{E}_{\vec{k}_1'} = \left(\frac{2\omega_{\vec{k}} - \Omega_{\vec{q}}}{\omega_{\vec{k}}}\right) \frac{l^2}{\hbar^6 \omega_{\vec{k}} \Omega_{\vec{q}} c_l^3 c_a} \left(\frac{v}{V}\right)^2 \times P_k^2 P_q \left| M^{E}_{\vec{k}_1'} + M'^{E}_{\vec{k}_1'} \right|^2 \delta_{\omega_{\vec{k}_1'}, 2\omega_{\vec{k}} - \Omega_{\vec{q}}} , \tag{24}$$

where

$$M^{E}_{\vec{k}_1} = \sum_{\vec{k}_2} \frac{2\omega_{\vec{k}_2} C_{\vec{k}_1'\vec{k}_2\vec{k}} D^{*}_{\vec{k}\vec{k}_2\vec{q}}}{(\omega_{\vec{k}_2})^2 - (\omega_{\vec{k}} - \Omega_{\vec{q}})^2} F(\vec{k}_1 - \vec{k}_2 - \vec{k}) f(\vec{k}_2 - \vec{k} + \vec{q}) , \tag{25}$$

$$M'^{E}_{\vec{k}_1'} = \sum_{\vec{k}_2'} \frac{2\omega_{\vec{k}_2'} C^{*}_{\vec{k}_2'\vec{k}\vec{k}} D^{*}_{\vec{k}_2'\vec{k}_1'\vec{q}}}{(\omega_{\vec{k}_2'})^2 - (2\omega_{\vec{k}})^2} F(\vec{k}_2' - 2\vec{k}) f(\vec{k}_1' - \vec{k}_2' + \vec{q}) .$$

III. DISCUSSION OF THEORETICAL RESULTS

The direct term $\mathcal{H}_1$ gives a result [Eq. (17)] which contains an over-all energy-conservation requirement and a single index-matching factor. It is difficult to estimate the relative strength of the direct contribution. In the work of Boyd *et al.*,[3] it apparently was appreciably larger than the higher-order contributions. In a case where the magnitude of $\vec{q}$ is too small to allow index matching (i.e., to allow both the condition $\vec{k}_1 = 2\vec{k} \pm \vec{q}$ and over-all energy conservation), the argument of f in Eq. (17) is a minimum when $\vec{k}$, $\mp\vec{q}$, and $\vec{k}_1$ are all collinear. In the present work, however, we are primarily interested in the case where $\vec{q}$ is approximately orthogonal to $\vec{k}$ and in the resonance effects which arise in second order.

There are obvious similarities between Eq. (14), which describes the generation of second-harmonic[8] optical radiation by consecutive SHG and Brillouin scattering processes, and Eq. (22), which describes the second-order phonon-assisted SHG process of interest here. In particular, we note the presence of the same C and D coefficients. The primary differences lie in (a) the fact that the first process requires a real intermediate state while the intermediate state is virtual for the second process and (b) the way the square modulus is taken; in the second process, there is interference between the two terms. Furthermore, we have an energy-conservation requirement in the first case, whereas there is a resonance denominator in the second, e.g.,

$$\delta_{\omega_{\vec{k}_1}, \omega_{\vec{k}} + \Omega_{\vec{q}}} \rightarrow \frac{2\omega_{\vec{k}_2} c_l / L}{(\omega_{\vec{k}_2})^2 - (\omega_{\vec{k}} + \Omega_{\vec{q}})^2} . \tag{26}$$

In the consecutive process, there are two energy-conservation conditions. In the virtual-intermediate-particle process of interest, however, we now have only one conserved quantity, which is the over-all energy, instead of two. Instead of the other energy-conservation requirement, we now have a resonance condition, which is satisfied at the *same* point as the conservation condition for the real-intermediate-particle case. The momentum-matching conditions are the same in both cases.

Since the real- and virtual-intermediate-particle cases are so similar, it is important to consider the relative strengths of the two contributions. Comparing, for example, the first terms in Eqs. (14) and (22), we find the ratio at resonance to be

$$\beta = |A_{\vec{k}_1}|^2 / |M^{A}_{\vec{k}_1}|^2 = \left| (L/c_l)(\omega_{\vec{k}_2} - \omega_{\vec{k}} - \Omega_{\vec{q}}) \right|^2_{\text{res}} . \tag{27}$$

If we treat the loss and linewidth effects by the common method of introducing a quantity $\frac{1}{2}\Gamma$ for the imaginary part of $\omega_{\vec{k}_2} - \omega_{\vec{k}} - \Omega_{\vec{q}}$ at resonance, we have

$$\beta = (\Gamma L / 2c_l)^2 . \tag{28}$$

Thus the virtual-intermediate-particle case will be the dominant term if

$$\Gamma < 2c_l / L . \tag{29}$$

Typically, $2c_l/L$ is in the order of 5×10^{10} sec^{-1}. The value of Γ to be used requires more careful selection. In essence,[8] the quantity $\frac{1}{2}\Gamma$ is the minimum value that $|\omega_{\vec{k}_2} - \omega_{\vec{k}}|$ can take when $\omega_{\vec{k}}$ is the frequency of a given laser quantum and $\omega_{\vec{k}_2} = \omega_\lambda(\vec{k}_2)$ is the dispersion relation for photons in the crystal. Thus, the laser linewidth is not a relevant quantity here, the main contribution to Γ being loss in the crystal. If the optical radiation intensity decays in the crystal as $e^{-\alpha x}$, then $\alpha = \Gamma/c_l$ and Eq. (29) becomes

$$\alpha L < 2 . \tag{30}$$

In other words, the virtual-intermediate-particle process of second-order perturbation theory is more important than the consecutive process if there is less than about 90% intensity loss as a photon propagates across the crystal.[9] In the experiments described in Sec. IV, the inequality $\alpha L \ll 1$ was satisfied, and thus the resonant process dominates.

Assuming that over-all energy conservation is satisfied, we have factors of the form [see, for example, Eqs. (22)–(25)]

$$\left| \frac{F(\vec{K}_1) f(\vec{K}_2)}{\omega_{\vec{k}_2} - \omega_0} \right|^2 , \tag{31}$$

which will be maximized. The question now arises as to which, if any, of the conditions

$$\vec{K}_1 = 0 ,$$

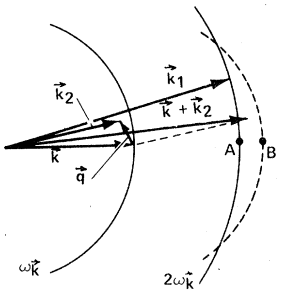

(a) MATCHING CONDITIONS FOR FIRST TERM

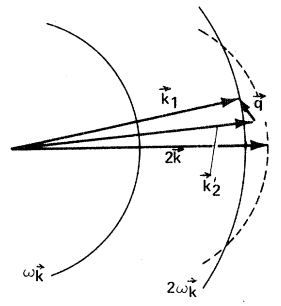

(b) MATCHING CONDITIONS FOR SECOND TERM

FIG. 2. Reciprocal-space representations of energy conservation and index matching [(a) $M^A_{\vec{k}1}$ and (b) $M^A_{\vec{k}1}$] when $\vec{\kappa}_2=0$ [see expression (31)] is satisfied. Points A and B are not coincident because the usual SHG index-matching condition is not assumed to be satisfied.

$$\vec{\kappa}_2=0\ ,\qquad \mathrm{Re}(\omega_{\vec{k}_2}-\omega_0)=0 \tag{32}$$

is more critical than the others. For $l\sim 1$ mm, $\Delta\kappa_2\sim 10\ \mathrm{cm}^{-1}$ is the half-width of the f function, and $\Delta\kappa_1\sim 1\ \mathrm{cm}^{-1}$ for $L\sim 1$ cm. The half-width of the resonance is $\Delta\omega\sim\frac{1}{2}\Gamma$. If we consider the first term in Eqs. (22) and (24), we have[8] $\omega_0=\omega_{\vec{k}}$ and, if $(\vec{k}_2-\vec{k})$ is parallel to $\vec{k}$, then $\Delta\omega\approx c_l\Delta k$ and the half-width is $\Delta k\sim\frac{1}{2}\alpha$. Thus $\Delta k\ll\Delta\kappa_{1,2}$, since $\alpha L\ll 1$ and $l<L$. In this case, the resonance condition would be the most stringent. However, if $(\vec{k}_2-\vec{k})$ is almost normal to $\vec{k}$, the frequency offset can be much smaller (i.e., $\Delta\omega\ll c_l\Delta k$). In fact, if $\vec{k}_2$ is on the same energy shell as $\vec{k}$ (see Fig. 2) and both photons belong to the ordinary branch, Δk can be as large as $2|\vec{k}|$ and still satisfy the condition $\omega_{\vec{k}_2}=\omega_{\vec{k}}$.

In the experiments mentioned in Sec. IV, it is not possible to satisfy both index-matching conditions ($\vec{\kappa}_1=0$, $\vec{\kappa}_2=0$) simultaneously, primarily because $|\vec{q}|$ is too small when the lithium-niobate crystal is 80 °C cooler than the SHG index-matching temperature.[10] Therefore, we may, in general, expect two peaks (i) where $\vec{\kappa}_1=0$ and $\omega_{\vec{k}_2}=\omega_0$ and (ii) where $\vec{\kappa}_2=0$ and $\omega_{\vec{k}_2}=\omega_0$. As noted,[10] however, case (i) does not occur for the second term of Eqs. (22) and (24) under the conditions currently being considered. Furthermore, the result of case (i) for the first term in Eqs. (22) and (24) is a photon emitted at the same angle as the noncollinearly generated 0.53-μ photons described elsewhere.[11] This would be difficult to detect in the ring that is thereby produced on an intersecting plane.[11,12] The detector in the experiments described in Sec. IV was placed at appreciably smaller angles than this. Thus, we are concerned with satisfying the conditions $\vec{\kappa}_2=0$, $\omega_{\vec{k}_2}=\omega_0$.

The situation for the first term ($\omega_0\equiv\omega_{\vec{k}}$) is shown in Fig. 2(a). The point $\vec{k}_1$ must lie on the $\omega=2\omega_{\vec{k}}$ surface to satisfy over-all energy conservation.[8] To satisfy the resonance condition, $\vec{k}_2$ must lie on the same shell ($\omega=\omega_{\vec{k}}$) as $\vec{k}$ and this requires a specific angle $\theta^A_{R_1}$ between $\vec{q}$ and the plane normal to $\vec{k}$. This angle is given by

$$\vec{q}^{\,2}-2|\vec{k}|\,|\vec{q}|\sin\theta^A_{R_1}=0\ , \tag{33}$$

$$\theta^A_{R_1}=\sin^{-1}(\tfrac{1}{2}\mu)\ , \tag{34}$$

where $\mu=|\vec{q}|/|\vec{k}|$. The vector length $|\vec{\kappa}_1|=|\vec{k}_1-(\vec{k}_2+\vec{k})|$ is a minimum (and thus F a maximum) when $\vec{k}_1$ is collinear with $\vec{k}+\vec{k}_2$; the angle between $\vec{k}_1$ and $\vec{k}$ is then also $\theta^A_{R_1}$.

The situation for the second term ($\omega_0\equiv 2\omega_{\vec{k}}$) is shown in Fig. 2(b). Again, $\vec{k}_1$ must lie on the $\omega=2\omega_{\vec{k}}$ surface. In the present case, $\vec{k}_2$ will also lie on the same surface at resonance. This will occur for an angle $\theta^A_{R_2}$ (between $\vec{q}$ and the plane normal to $\vec{k}$) which is given approximately[13] by

$$\theta^A_{R_2}=\sin^{-1}(\tfrac{1}{4}\mu)\ . \tag{35}$$

We note that, for the second term, F is maximized when $\vec{k}_2$ is parallel to $\vec{k}$, and the angle between $\vec{k}_1$ and $\vec{k}$ is then approximately[13] equal to $\theta^A_{R_1}$, the same output angle as for the first term. Therefore, the angle of emission of the final photon is essentially[13] the same for both terms in Eq. (22). However, as shown by Eqs. (34) and (35), the angle of acoustic propagation for which resonance occurs is quite different in the two cases. This is because the magnitude of the optical wave vectors connected by the wave vector $\vec{q}$ is approximately twice as large for the second term (see Fig. 2).

In the foregoing discussion, we have so far ignored the presence of the stimulated phonon-emission process described by Eq. (24). In this case, $\vec{q}\to-\vec{q}$ and $\Omega_{\vec{q}}\to-\Omega_{\vec{q}}$. Equations (33) and (34) yield $\theta^E_{R_1}=-\sin^{-1}(\frac{1}{2}\mu)$ and $\theta^E_{R_2}=-\sin^{-1}(\frac{1}{4}\mu)$, and the angle between the optical input $\vec{k}$ and the output $\vec{k}_1$ is also $\theta^E_{R_1}=-\theta^A_{R_1}$. Thus, two output beams would be observed, one at $+\sin^{-1}(\frac{1}{2}\mu)$ and the other at $-\sin^{-1}(\frac{1}{2}\mu)$. Each would show a resonance at two different angles between $\vec{q}$ and the plane normal to $\vec{k}$ [e.g., for the output beam at $+\sin^{-1}(\frac{1}{2}\mu)$ these resonance angles would be $+\sin^{-1}(\frac{1}{2}\mu)$, $+\sin^{-1}(\frac{1}{4}\mu)$]. However, if the acoustic wave were a *standing* wave rather than a traveling wave (i.e., if there were as many $-\vec{q}$ phonons as $+\vec{q}$ phonons), each output beam

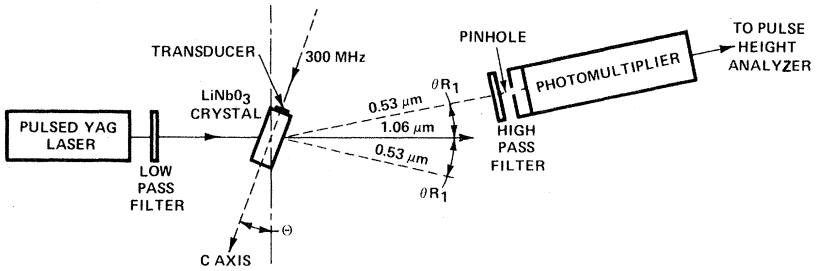

FIG. 3. Experimental measurement of resonant phonon-assisted second-harmonic generation.

would show all four resonances, since absorption of a phonon $\vec{q}$ and emission of a phonon $-\vec{q}$ give the same photon output angle when f is maximized.

In summary, if the SHG output at an angle of either $\pm\sin^{-1}(|\vec{q}|/2|\vec{k}|)$ is measured as a function of the angle between $\vec{q}$ and the normal to $\vec{k}$ at temperatures well below the index-matching temperature, either two or four resonance peaks may be observed, depending on whether the acoustic wave is a traveling or standing wave. The resonant peaks as a function of angle are due to the traversal of a path in the ω plane close to poles in the scattering amplitude at $\pm\omega_{\vec{k}}$ and $\pm 2\omega_{\vec{k}}$, as given by Eqs. (23) and (25). For a standing acoustic wave, the values of the angle between $\vec{q}$ and the plane normal to $\vec{k}$ for which a resonance is expected are $\pm\sin^{-1}(\frac{1}{2}\mu)$ and $\pm\sin^{-1}(\frac{1}{4}\mu)$, i.e., with separations of $\frac{1}{4}\mu$, $\frac{1}{2}\mu$, and $\frac{1}{4}\mu$ between them if $\mu \ll 1$.

IV. EXPERIMENT

Phonon-assisted SHG was first observed[3] in (cubic) GaAs, where the birefringence which is necessary for the usual index-matched SHG is absent. In these experiments, the optical- and acoustic-propagation vectors were collinear. In the experiments reported in this article, we utilize lithium niobate, which is birefringent and in which index-matched SHG is readily obtained. The main advantage of lithium niobate is that the conical SHG output which is observed[11] below the index-matching temperature gives very accurate information on the refractive indices and proximity to index matching. In the present experiments, the acoustic- and optical-propagation vectors are far from collinear, in order to observe the resonance behavior discussed earlier.

A. Experimental Arrangement

The experimental arrangement is shown in Fig. 3. A $10\times5\times5$-mm^3 $LiNbO_3$ crystal (c axis along the long dimension) was polished, and an evaporated CdS transducer (3 mm diam) generating longitudinal waves was placed on one of the square faces. The transducer was excited by an rf oscillator near 300 MHz via an impedance-matching network. Because the square faces were highly polished, the acoustic reflection at the ends was high, and thus the acoustic wave was almost a pure standing wave along the c axis. This high Q of the lithium-niobate crystal resulted in sharp resonant dips in the impedance of the crystal as seen by the oscillator, and the experiments were carried out with the oscillator frequency held fixed at the center of one of these acoustic resonances, close to 300 MHz. Besides increasing the energy density in the acoustic standing wave in the crystal, the resonant effects had the further advantage of reducing the effect of off-axis acoustic emission from the transducer since this "walks off" the end faces.

The optical input radiation was obtained from a TRG 400 series neodymium: yttrium-aluminum-garnet (Nd: YAG) laser repetitively pulsed via a rotating-prism Q switch at 1.06 μ in the lowest-order (TEM_{00}) transverse mode. An intracavity barium-sodium-niobate crystal regularly used for doubling the 1.06-μ laser radiation was retained in the cavity (but not heated to its SHG index-matching temperature) in order to polarize the output.[14] The laser radiation was optically filtered to remove any second-harmonic and pump radiation in the visible region. The polarized 1.06-μ radiation was coupled into the lithium-niobate crystal as an ordinary wave. The $LiNbO_3$ crystal was placed in a gimbal mount and held at room temperature (compared with an SHG matching temperature of $\simeq 100\,^\circ$C). The angle between the 1.06-μ beam and the long dimension of the crystal (and thus the acoustic beam) could be varied over the range $(90\pm6^\circ)$. The loss in the crystal was much less than 1 cm^{-1} at both 0.53 and 1.06 μ and thus $\alpha L \ll 1$ [see Eq. (30)].

The detector for the 0.53-μ acoustically induced doubled radiation consisted of an optical filter, a photomultiplier, and a 200-μ-diam pinhole, set at the appropriate angle to the incoming optical beam and at a distance of about 30 cm from the crystal. An infrared-absorbing filter was used to reduce the scattered 1.06-μ radiation. The pinhole position was slightly readjusted for maximum average signal after each change in crystal orientation, primarily because of the small shift due to refraction. Because of fluctuations in the laser output, the photomultiplier pulses were fed to 100 channels of a pulse-height analyzer so that the 0.53-μ height distribution was available for analysis.

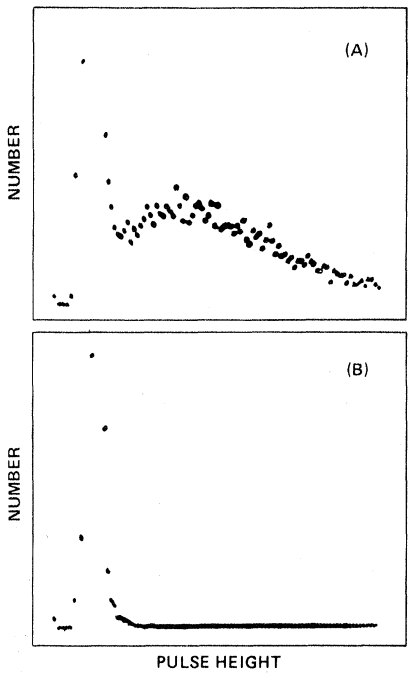

FIG. 4. Photomultiplier pulse-height distributions: (a) typical distribution of assisted second-harmonic pulses and (b) distribution in the absence of acoustical radiation.

B. Results

A typical pulse-height distribution for the acoustically induced radiation is shown in Fig. 4(a). The first peak is due to small noise pulses, as indicated by Fig. 4(b), which shows the pulse-height distribution in the absence of acoustic radiation. In Fig. 5, two parameters deduced from these data, the mean induced pulse height and the most probable height, are plotted against the angle of rotation of the lithium-niobate crystal (and thus the angle of the acoustic beam) with respect to the incoming laser beam. We note that both parameters, derived from the data in different ways, show a double resonance peak. The two peaks are just resolved and are separated by approximately $\Delta\Theta = 1.2^\circ$ of arc in terms of crystal rotation. As shown in Sec. III, we expect possible resonance peaks at values of θ (the angle between $\vec{q}$ and the normal to $\vec{k}$ of $\pm\sin^{-1}(\frac{1}{4}\mu)$ and $\pm\sin^{-1}(\frac{1}{2}\mu)$, where $\mu = |\vec{q}|/|\vec{k}|$. The parameter μ is given by

$$\mu = \lambda_0/\lambda_a = \lambda_0\nu_a/c_a\,, \tag{36}$$

where λ_0 and λ_a are the wavelengths of the fundamental optical and acoustic radiation in the crystal and ν_a is the acoustic frequency. In the present experiments, the wavelength λ_0 is

$$(1.06\times10^{-4})/2.24\ \text{cm} = 0.48\times10^{-4}\ \text{cm}.$$

The longitudinal sound velocity in $LiNbO_3$ is[15] $7.43\times10^5\ \text{cm sec}^{-1}$ and $\nu_a = 3\times10^8\ \text{sec}^{-1}$. Hence

$$\mu = 0.0192\,. \tag{37}$$

We note that the crystal rotation angle Θ and the angle θ between $\vec{q}$ and the plane normal to $\vec{k}$ are not equivalent, due to the refraction which takes place at the crystal surface. Thus

$$\sin\theta = \sin\Theta/2.24 \tag{38}$$

by Snell's law. Hence, the angle $\Delta\Theta = (1.2\pm0.05^\circ)$ is equivalent to $\Delta\theta = (0.535\pm0.025^\circ)$. From Eq. (37), the angle given by $2\sin^{-1}(\frac{1}{2}\mu)$ is 1.10° and that given by $2\sin^{-1}(\frac{1}{4}\mu)$ is 0.55°. The latter value is in good agreement with the observed $\Delta\theta$ of $(0.535\pm0.025)^\circ$. The double resonance peak shown in Fig. 5 is therefore interpreted as being due to the (a) phonon-absorption and (b) stimulated phonon-emission contributions which are resonant at $\omega_{\vec{k}_2} = 2\omega_{\vec{k}}$ when $\theta_{R_2} = \pm\sin^{-1}(\frac{1}{4}\mu)$, respectively. In other words, the two peaks are due to the pole at $\omega_{\vec{k}_2} = 2\omega_{\vec{k}}$ in the second terms in Eqs. (22) and (24). The other two peaks which are to be expected at $\theta_R = \sin^{-1}(\frac{1}{2}\mu)$ were

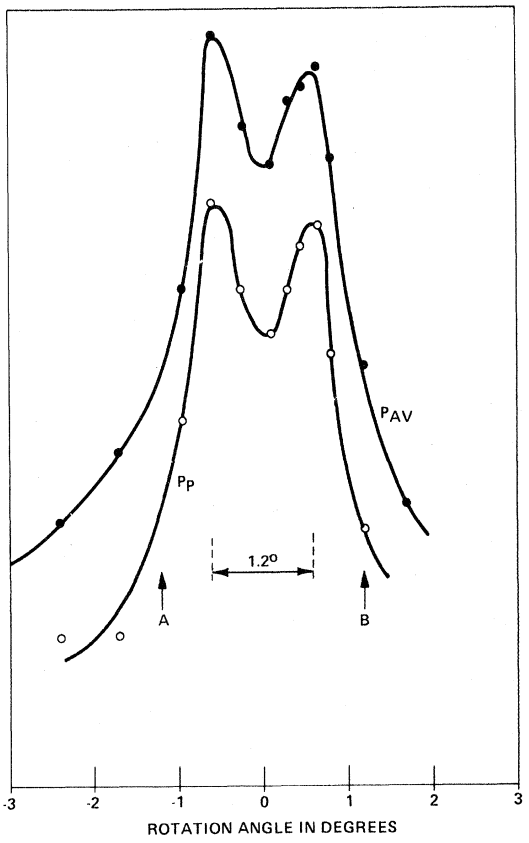

FIG. 5. Phonon-assisted second-harmonic output, in arbitrary units, as a function of the angle of rotation of the crystal. The average power output P_{AV} (black dots) and most probable pulse-height P_P (open circles) are shown.

not observed, presumably because either the strength is lower or the resonance width is appreciably greater (i.e., the pole at $\omega = \omega_{\vec{k}}$ is further from the real axis). The angular positions at which these peaks would occur are shown by arrows A and B in Fig. 5.

V. SUMMARY

A quantum approach to phonon-assisted (or acoustically induced) optical-harmonic generation based on perturbation theory has been developed. The results obtained in second order suggest that resonant behavior may be observed if the acoustic beam is almost normal to the optical beam. This possibility is studied experimentally in $LiNbO_3$ with a 1.06-μ optical fundamental and 300-MHz longitudinal acoustic wave. A double resonance peak is observed, with a separation of 1.2° in the rotational position of the crystal. This separation agrees closely with the expected separation of $\frac{1}{2}\mu$ between resonances due to the pole at $2\omega_{\vec{k}}$ for the two processes of absorption and stimulated emission of phonons. Two more resonances which could occur (due to the pole at $\omega_{\vec{k}}$) have not been observed.

ACKNOWLEDGMENTS

The authors are indebted to Dr. G. H. Azarbayejani for providing excellent lithium-niobate crystals, R. F. Steinberg for the transducer work, and to D. M. Shupe and Dr. R. K. Mueller for useful discussions.

*Present address: Hasler A. G., Bern, Switzerland.

[1]P. A. Franken, A. E. Hill, C. W. Peters, and G. Weinreich, Phys. Rev. Letters 7, 118 (1961).

[2]S. E. Harris, R. W. Wallace, and G. F. Quate, IEEE J. Quantum Electron. QE-4, 354 (1968).

[3]G. D. Boyd, F. R. Nash, and D. F. Nelson, Phys. Rev. Letters 24, 1298 (1970).

[4]D. F. Nelson and M. Lax (unpublished).

[5]C. Y. She, Phys. Rev. 176, 461 (1968).

[6]See, for example, A. Yariv, *Quantum Electronics* (Wiley, New York, 1967), Chap. 21; N. Bloembergen, *Nonlinear Optics* (Benjamin, New York, 1965), Chap. 4 and references therein.

[7]See, for example, P. Roman, *Introduction to Quantum Field Theory* (Wiley, New York, 1969), Chap. 4.

[8]It should be noted that $2\omega_{\vec{k}}+\Omega_{\vec{q}}$ is essentially the true second harmonic since $\Omega_{\vec{q}} \sim 10^{-6}\omega_{\vec{k}}$ for ~300-MHz phonons. Similarly, $\omega_{\vec{k}}+\Omega_{\vec{q}} \approx \omega_{\vec{k}}$ to a high degree of accuracy.

[9]It should be noted that the converse does not necessarily apply, because Eq. (14) is invalid when αL is not small. In fact, the first term in Eq. (14) decreases as $(\alpha L)^{-3}$ when αL is large.

[10]For the same reason, it is not possible to satisfy both $\vec{\kappa}_1 = 0$ and $\omega_{\vec{k}2} = 2\omega_{\vec{k}}$ (i.e., for the second term), although $\omega_{\vec{k}2} = 2\omega_{\vec{k}}$ and $\vec{\kappa}_2 = 0$ can be satisfied simultaneously.

[11]J. A. Giordmaine, Phys. Rev. Letters 8, 19 (1962); C. Deutsch, D. M. Shupe, and P. N. Keating, Bendix Tech. J. 2, 101 (1969).

[12]It is worth noting here that experimental data for conventional SHG and Brillouin scattering indicates that in practice the F requirement is usually less stringent than the f requirement. This is probably due to the importance of refractive-index inhomogeneities in the SHG process.

[13]These results are approximate because the usual SHG index-matching conditions are not satisfied (i.e., the points A and B in Fig. 2 are not coincident). However, the approximation is usually a very good one.

[14]J. F. Geusic, H. J. Levinstein, S. Singh, R. G. Smith, and L. G. Van Uitert, Appl. Phys. Letters 12, 306 (1968).

[15]E. G. Spencer, P. V. Lenzo, and K. Nassau, Appl. Phys. Letters 7, 67 (1965).

PHYSICAL REVIEW B VOLUME 3, NUMBER 10 15 MAY 1971

Free Energies of Vacancies and Rare-Gas Crystal Mixtures

H. R. Glyde
Chalk River Nuclear Laboratories, Atomic Energy of Canada Limited, Chalk River, Ontario, Canada
(Received 21 December 1970)

The Gibbs-Bogolyubov variational principle is used to calculate the free energy of vacancy formation $g_v(T)$ in solid Kr, Ne, and Cu and the interchange parameter w for dilute Ar-Kr mixtures. These calculations include vibrational properties and, since any temperature can be considered, all other thermal properties can be obtained. For the vacancy, the formation energy obtained in this way as $h_v = g_v - (dg_v/dT)_P T$ is essentially the same as expected from equivalent static-lattice calculations at $T = 0$ °K. Thus, the vibrational motion does not encourage further relaxation and there remains a large discrepancy between computed and observed h_v in solid Kr, although the entropies s_v compare well. The computed w's agree very well with the observed values of Fender and Halsey.

I. INTRODUCTION

Most calculations of point-defect properties such as the formation energy[1-4] or substitutional energy are done for $T = 0$ °K only. This is because (a) a static vibration-free lattice is considered and (b)